

In Vivo Analysis of Growth Hormone Receptor Signaling Domains and Their Associated Transcripts

Jennifer E. Rowland,^{1,2†} Agnieszka M. Lichanska,^{1†} Linda M. Kerr,¹ Mary White,²
Elisabetta M. d’Aniello,¹ Sheryl L. Maher,¹ Richard Brown,¹ Rohan D. Teasdale,¹
Peter G. Noakes,² and Michael J. Waters^{1*}

*Institute for Molecular Bioscience¹ and School of Biomedical Sciences,² University of Queensland,
St. Lucia, Queensland, Australia*

Received 16 June 2004/Returned for modification 4 August 2004/Accepted 23 September 2004

The growth hormone receptor (GHR) is a critical regulator of postnatal growth and metabolism. However, the GHR signaling domains and pathways that regulate these processes in vivo are not defined. We report the first knock-in mouse models with deletions of specific domains of the receptor that are required for its in vivo actions. Mice expressing truncations at residue m569 (plus Y539/545-F) and at residue m391 displayed a progressive impairment of postnatal growth with receptor truncation. Moreover, after 4 months of age, marked male obesity was observed in both mutant 569 and mutant 391 and was associated with hyperglycemia. Both mutants activated hepatic JAK2 and ERK2, whereas STAT5 phosphorylation was substantially decreased for mutant 569 and absent from mutant 391, correlating with loss of IGF-1 expression and reduction in growth. Microarray analysis of these and GHR^{-/-} mice demonstrated that particular signaling domains are responsible for the regulation of different target genes and revealed novel actions of growth hormone. These mice represent the first step in delineating the domains of the GHR regulating body growth and composition and the transcripts associated with these domains.

Over the last decade, extensive in vitro studies have identified signaling pathways triggered by growth hormone receptor (GHR) activation and the sequence motifs within the conserved cytoplasmic domain of the receptor that are required to initiate these pathways. These studies have established the critical signaling role of JAK2 tyrosine kinase, which is recruited to the trimeric GHR2:GH complex at the box 1/2 motif (9). Hormone binding initiates JAK2 transphosphorylation and activation, resulting in phosphorylation of critical tyrosines within the cytoplasmic domain of the GHR, as well as other direct JAK2 substrates such as IRS-1 and -2. The distal cytoplasmic phosphotyrosines of GHR have been shown to recruit signal transducer and activator of transcription 5 (STAT5) and other proteins through SH2-domain interactions, whereas the proximal JAK2 activation domain is responsible for ERK1/2 and phosphatidylinositol 3-kinase (PI 3-kinase) activation (30), although it has been claimed that residues distal to m390 are required for ERK1/2 activation (residue 390, mouse sequence numbers given throughout) (38). There is some dispute regarding the distal tyrosine residues used to recruit STAT5 for activation, notably in relation to tyrosine m498 (8, 33); moreover, it has been claimed that tyrosines m341 and m346, proximal to boxes 1 and 2, may also generate active STAT5 (31).

In vitro studies have identified other signaling elements within the distal region of the GHR cytoplasmic domain, for example, a JAK2-independent calcium signaling element between residues m465 and m517 (30). SHP2 phosphatase can have a dual role when bound to the cytoplasmic domain of the

GHR. It binds primarily to m606 to attenuate JAK2-STAT5 signaling but can also serve as an adaptor protein (30). GH-driven activation of STAT5 can also be attenuated by suppressor of cytokine signaling proteins (SOCS proteins). Tyrosine m498 and other proximal tyrosines are reported to bind SOCS-3, whereas residues m569 to m650 bind to other SOCS proteins, SOCS-2, and CIS (25). These SOCS proteins are believed to inhibit GH-induced gene transcription by competing with STAT5.

The relevance of these extensive in vitro studies to the in vivo state has not been established. Until the very recent publication by Milward et al. (19), there have been no publications of inactivating clinical mutations within the conserved 352 residue cytoplasmic domain of the GHR, other than an intron 9 donor splice mutation that effectively removes the cytoplasmic domain (1). STAT5b-deficient (STAT5b^{-/-}) mice show a reduction in circulating IGF-1 (the central mediator of the growth actions of GH), and STAT5 response elements have recently been identified within the IGF-1 promoter (5, 35, 37, 41). One would predict that removal of tyrosines critical for docking of STAT5 would drastically reduce *Igf1* transcript and consequently IGF-1 in serum, leading to reduction in postnatal growth. However, although STAT5^{-/-} mouse models do display growth retardation, this retardation is not as extensive as that seen in GHR gene-disrupted (GHR^{-/-}) mice (4), indicating that other signaling pathways must play a significant physiological role in potentiating the growth signaling response of GHR. Moreover, the basis for regulation of the many other physiological roles of GH, such as the regulation of fat and carbohydrate metabolism, reproduction, bone turnover, and extended life span, need to be delineated in vivo by receptor mutation analysis. This is particularly relevant given that the sexual dimorphism in secretory pattern of GH is known to be

* Corresponding author. Mailing address: Institute for Molecular Bioscience, University of Queensland, St. Lucia, Brisbane, Queensland 4072, Australia. Phone: (61) 7-33462037. Fax: (61) 7-33462101. E-mail: m.waters@uq.edu.au.

† J.E.R. and A.M.L. contributed equally to this study.

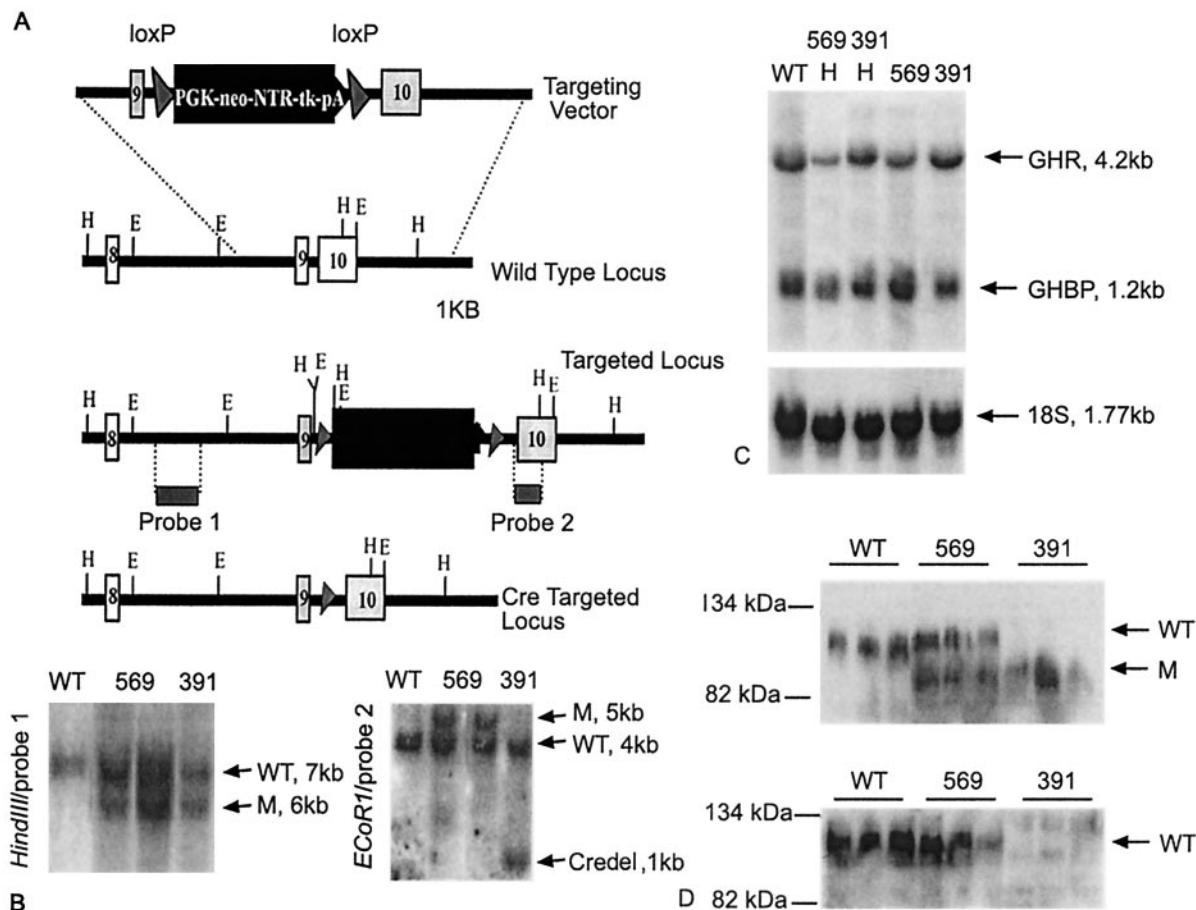


FIG. 1. Creation of GHR targeted knockin lines. (A) Targeting strategy for both mutant types with altered exon 10 using neomycin resistance for selection in ES cells. A Cre/lox system was adapted to remove the selection cassette. (B) Southern confirmation of heterozygous ES cell clones for mutant 569 (1), mutant 391 (2), and mutant 391 transiently transfected with Cre recombinase (3). (C) Northern blot analysis confirmed that *Ghr* and *Ghrbp* (GH-binding protein) mRNA was expressed in hepatic tissue in both mutants 569 and 391 in both heterozygous (H) and homozygous forms. (D) Western blotting of hepatic microsomal membranes with cytoplasmic domain specific antibody detected truncated mutant 569 GHR protein; however, the epitope was absent from mutant 391.

responsible for the sexual dimorphism of many processes in rodents, particularly hepatic metabolism (34).

Here we report the creation and characterization of the first knockin mouse models designed to determine how and which specific regions of the GHR cytoplasmic domain are required for GH actions observed in vivo. Our phenotypic and microarray analyses with these mutant mice demonstrate that residues distal to m391 are critical for postnatal growth, STAT5 phosphorylation, and IGF-1 activation. However, in the liver the majority of regulated transcripts, including those for several novel GH actions, are associated with the proximal JAK2 activation domain.

MATERIALS AND METHODS

Gene replacement strategy. The GHR cytoplasmic domain was modified by homologous recombination with the GHR locus encompassing exons 9 and 10. Two targeting constructs were designed and generated incorporating a short homology arm of 1.4 kb upstream of exon 9 and a long homology arm of 4 kb, including exon 10 and the downstream intronic sequence.

Construction of targeting vector. Probes for the exon 9 and 10 portions of the GHR were generated by synthetic oligonucleotide creation (Genset Oligos, Lismore, Australia) or by PCR, respectively (10F, 5'-CCTGGGTCGAGTT

CATTGAGC-3', 10R10, 5'-GCCCACTTACACCACCCAGC-3', 1-kb exon 10 product).

A 16-kb Sau3A1 fragment containing exons 9 and 10 of the mGHR gene was isolated from a 129/SVJ mouse genomic λ phage library (Stratagene, La Jolla, Calif.). A 6.4-kb portion of this that contained exons 9 and 10 with a flanking intronic sequence was cloned into pBluescript by XbaI to use for targeting to embryonic stem (ES) cells (GenBank accession number AY271378). This fragment was subjected to QuikChange mutagenesis (Stratagene) to introduce relevant mutations to exon 10. Clone 1 was created by two rounds of mutagenesis to truncate the mature GHR at residue 569 (forward, 5'-GCA TGG AAGCCACGTCCTGTATAAAATAGAGCTTTAACCAAGAGG-3'; reverse, 5'-CCTCTTGGTTAAAGCTCTATTTTATACAAGACGTGGCTTCCATGC-3') and convert Y539/545-F (forward, 5'-CTGCCAAGAAAATTTCAGCATGAACAGCGCCTTCTTTGTGAGTC-3'; reverse, 5'-GACTCA CAAAAGAAGGCGCTGTTCATGCTGAAATTTTCTTGGCAG-3'). Clone 2 was treated to one round of mutagenesis to result in truncation of the mature GHR at residue 391 (forward, 5'-GCTGGTATCCTTGGAGCCTAGGATGATGATTCTGGGCG-3'; reverse, 5'-CGCCAGAAATCATATCCTAGGCTCCAAGGATACCAGC-3'). Both mutants were confirmed by automated sequence analysis (AGRF, University of Queensland, St. Lucia, Queensland, Australia). A floxed selection cassette (PGKneoNTRtkpA) (42) was then inserted between exons 9 and 10 by BamHI and XbaI engineered restriction sites (Fig. 1A).

Production of gene targeted mice. Targeting vector plasmids were linearized by NotI digest (cutting immediately upstream of the 5' flanking short arm) and purified by GeneClean II (Qiogene, Carlsbad, Calif.) prior to electroporation.

The vector was electroporated into low-passage 129/SVJ agouti ES cells, and homologous recombinants were selected for by G418 resistance, followed by genotyping. Positive heterozygote recombinants were Cre deleted by transient transfection with pMC-Cre (7) to remove the PGKneoNTRtkpA selection cassette from the genome. ES cells minus the selection cassette but retaining the desired GHR mutations (569 and 391) were confirmed by Southern blotting (described below). Cre-deleted ES cells were then injected into C57 black blastocysts and implanted in pseudopregnant foster mothers housed in a specific-pathogen-free facility. Chimeric offspring were mated with C57 black mice to produce germ line heterozygote offspring. Some chimeras were generated by injection of heterozygote ES cells that had not been Cre deleted. In this case, Cre deleter transgenic mice were obtained (29), which ubiquitously express Cre recombinase enzyme. These were mated with the F₁ germ line mice and the chimeric males, which still carried the selection cassette.

Genotyping strategies. Southern blotting was used for genotyping as described previously (28). HindIII-digested genomic DNA was electrophoresed, transferred to a nylon membrane (Hybond N+; Amersham Pharmacia, Sydney, Australia), and hybridized to a probe corresponding to a 1.4-kb HincII/XbaI fragment of upstream external intron 8/9 of the murine GHR. The probe was labeled with [α -³²P]dCTP by random priming with a commercially available kit (Megaprime DNA Labeling Systems; Amersham Pharmacia). The 7-kb fragment corresponded to the wild-type (WT) locus, whereas a 6-kb fragment was observed for the targeted locus (Fig. 1B, left panel). Analysis of Cre recombination was performed identically with the exception of EcoRI restriction digest, followed by hybridization to a probe corresponding to exon 10 as described earlier. In this case the WT locus yielded a 4.3-kb band, the targeted locus yielded a 5.3-kb band, and the Cre-deleted targeted locus yielded a 1-kb band (Fig. 1B, right panel).

Animals. Animals were housed in an approved facility and treated in accordance with university guidelines, and all procedures were approved by the University of Queensland Animal Ethics Committee and the Australian Office of the Gene Technology Regulator. Water and feed pellets were available ad libitum under a 12-h light-dark cycle at 20 to 22°C. Fasting of the animals was performed overnight (16 h) with animals having water ad libitum. All animals passed standard virus screens quarterly throughout.

IGF-1 measurements. Acid ethanol-extracted serum IGF-1 was measured by using an IGF-1 radioimmunoassay kit (Bioclone, Sydney, Australia) according to the manufacturer's instructions.

RNA extraction and Northern blot analysis. Liver RNA samples from 42-day-old mice were isolated by using RNA-Bee reagent (Tel-Test, Inc., Friendswood, Tex.). Samples were separated on a denaturing gel (28) in morpholinepropane-sulfonic acid buffer and transferred onto an MSI membrane (Micron Separations, Westborough, Mass.). Hybridizations were performed by using Northern Max (Ambion, Austin, Tex.) and [α -³²P]dCTP-labeled (Megaprime Labeling Systems; Amersham Pharmacia) cDNA probes. The rat IGF-1 cDNA was kindly provided by Adrian Herington (QUT, Brisbane, Australia). The mouse GHR cDNA was kindly provided by Frank Talamantes (University of California, Santa Cruz, Calif.), and a probe encompassing exons 2 to 7 was prepared from this cDNA by restriction digest with HindIII and EcoRV. Probes for *Sih2*, *Es31*, *Ang*, *Socs2*, and *Csad* were generated by reverse transcription-PCR with primers amplifying the same sequence as that targeted by Affymetrix oligonucleotide probe sets.

The loading control hybridization was performed with an 18S specific oligomer 5'-CATGGTAGGCACGGCGACTACCATC-3' (Genset Pacific, Pty., Ltd.) or a 150-bp fragment of 28S cDNA.

Microarray analysis. Liver samples from mice were dissected directly into RNAlater solution (Ambion), and total RNA was extracted by using an RNAqueous kit (Ambion) according to the manufacturer's instructions; the quality of the RNA was confirmed by spectrophotometry and gel electrophoresis (a compilation of samples, their codes, and their accession numbers is available at <http://research.imb.uq.edu.au/~mwaters/ghr/>). Samples from GHR^{-/-} mice were further purified by using LiCl precipitation before cDNA synthesis. A total of 5 μ g of the total RNA was used in the double-spaced cDNA synthesis by use of a MessageAmp kit (Ambion); the procedure was performed according to the manufacturer's instructions. The in vitro transcription reaction was performed by using an Enzo kit (Affymetrix, Santa Clara, Calif.) according to the manufacturer's instructions (except for increasing the reaction time to 14 h), and 15 μ g of cRNA was used to hybridize to an Affymetrix U74v2A array for 16 h. The arrays were subsequently washed and stained on the fluidic station and scanned on a confocal scanner (Affymetrix). The results were analyzed by using MAS 5.0 and the Data Mining Tool (DMT; Affymetrix). Each sample was processed by using Affymetrix MAS 5.0 software to visually check the array image and grid alignment and to compute signal values for each probe. Preliminary data analysis was applied to normalize the results by using global scaling to a set value of 100.

Furthermore, quality control analysis by using the spikes, percent present, internal control of 3'/5' ratios for β -actin and *Gapdh*, noise, and background was performed before further analysis was undertaken. The increases and decreases, as well as the signal log ratios (SLRs; equivalent to fold changes) were identified with MAS 5.0, and then the comparisons were loaded into DMT (Affymetrix), which allowed identification of transcripts changing in the same direction and the number of comparisons in which they change. In our case three separate mice were analyzed for each experimental group, allowing nine separate comparisons with another group (<http://research.imb.uq.edu.au/~mwaters/ghr/>). DecisionSite 7.2 for Functional Genomics and DecisionSite Statistics software (Spotfire, Somerville, Mass.) was used for clustering and statistical analyses on the samples. Genes that were called absent were eliminated from the initial comparisons. These were later reanalyzed, and the transcripts changing from absent in one group to present in the other were scored as increases, while the ones changing from present to absent were scored as decreases. Finally, a gene was scored as significantly changed in one group in comparison to the other if it was changed in the same direction in at least eight of nine comparisons performed and the fold change was >1.5.

Gene ontology (GO) classification was used to assign transcripts into functional groups by using the GO browser through the NetAffx at Affymetrix; to generate Table 3 we used only single GO terms (a full classification of the transcripts is available at <http://research.imb.uq.edu.au/~mwaters/ghr/>). All of the gene names reported in the present study are MGI approved and details about them can be found through the MGI website (<http://www.informatics.jax.org/>) or through the NCBI website (<http://www.ncbi.nlm.nih.gov/>).

Accession numbers for microarray data. The microarray data presented here has been submitted to a public database, and the accession numbers have been obtained from GEO (<http://www.ncbi.nlm.nih.gov/geo/>): GSM15488, GSM15489, GSM15490, GSM15491, GSM15492, GSM15493, GSM15494, GSM15495, GSM15496, GSM15497, GSM15498, and GSM15499 (<http://research.imb.uq.edu.au/~mwaters/ghr/>).

Western ligand blotting. Recombinant rat IGF-1 (Groppe, Adelaide, South Australia, Australia) was iodinated by the iodogen method and purified by using Sephadex G-50 chromatography. Western ligand blotting was performed as described previously (12), and blots were analyzed by densitometry. Relative ¹²⁵I-IGF-1 bound to IGFBPs was calculated from the integrated optical density value per sample. Bands at 38.5 to 41.5, 32 to 34, and 30 kDa correspond to IGF-binding protein 3 (IGFBP-3); IGFBP-1, -2, and -5; and IGFBP-4, respectively (12).

Immunoprecipitation and immunoblot analysis. Immunoblot analysis for JAK2, STAT5, and ERK1/2 phosphorylation was carried out on hepatic homogenates obtained from 19-day-old mice injected intraperitoneally with 4 μ g of bovine GH (bGH; Monsanto Company, St. Louis, Mo.)/g (body weight) and sacrificed 15 min later. Liver homogenates were used in immunoprecipitation with JAK2 (sc-278) and STAT5 (sc-835) antibodies from Santa Cruz Biotech (Santa Cruz, Calif.), and samples were separated on a polyacrylamide gel, blotted onto a nitrocellulose membrane, and probed with antiphosphotyrosine 4G10 antibody. ERK1/2 immunoblots were performed according to the information sheet accompanying the Phospho-p44/42 mitogen-activated protein kinase (Thr202/Tyr204) antibody from Cell Signaling Technology (catalog no. 9101) (Beverly, Mass.). The only exception to the protocol was that 2% (wt/vol) bovine serum albumin (fraction V; ICN, Aurora, Ohio) was used instead of 5% nonfat skim milk powder for incubation with the antibodies. Immunoblots were also carried out for HNF1, -3 β , and -6 (sc-6554 and sc-6559; Santa Cruz Biotech) with samples of adult liver by using immunoprecipitation and blotting with a second species of antibody, with normalization by protein loading, and by reprobing for the primary antibody. Loading control was performed by using immunoprecipitation antibody (JAK2 and STAT5) or ERK1 (sc-93; Santa Cruz Biotech). Proteins were detected by using ECL Plus Western blotting reagent (Amersham) according to the manufacturer's instructions. Bands on film were quantified with a Bio-Rad imaging densitometer GS-700 and software.

GHR measurements. Immunoblot analysis for GHR in liver membranes from 42-day-old mice was carried out according to the method of Lobie et al. (15) with a polyclonal antibody raised against a glutathione S-transferase fusion of the rabbit GHR cytoplasmic domain. Ligand binding with ¹²⁵I-bovine GH was carried out according to the method of Waters and Friesen (40).

RESULTS

Targeted mutation of the GHR. To elucidate the role of the GHR cytoplasmic domain sequence motifs and their target signaling cascades in manifesting the in vivo actions of GH,

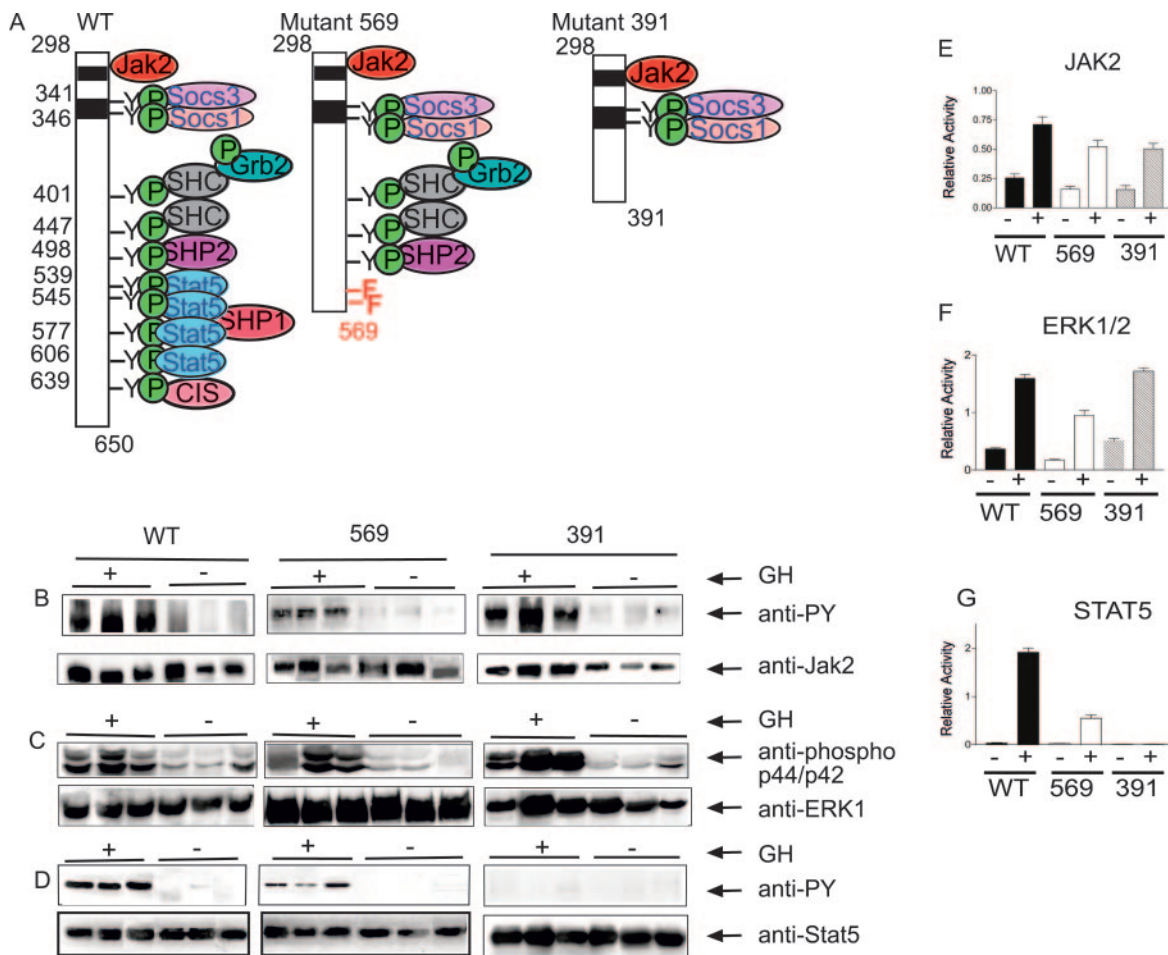


FIG. 2. Signaling in mutant mice in response to GH injections. (A) Predicted binding of signaling and adaptor molecules to the cytoplasmic domain of the GHR of the WT, mutant 569, and mutant 391. (B to D) Livers from the bGH- and saline-injected 19-day-old mice were used in immunoprecipitation analyses 15 min after the injections. Loading for each of the proteins was confirmed by using antibodies specific for an appropriate protein. (B) Antiphosphotyrosine (PY) immunoblot of JAK2 immunoprecipitated from liver homogenate. (C) Immunoblot for active ERK1/2 (Phospho-p44/42 mitogen-activated protein kinase) from liver homogenate. (D) Antiphosphotyrosine (PY) immunoblot of STAT5 immunoprecipitated from liver homogenate. (E to G) Densitometric quantification of the blots from panels B to D. Signals for the activated JAK2 (E), ERK1/2 (F), and STAT5a/b (G) were normalized for loading. The data for all graphs are presented as means \pm the SEM.

knockin mice bearing cytoplasmic domain mutations through targeted homologous recombination in ES cells were created (Fig. 1A). The resulting mice express murine GHR proteins either truncated at proline m569, together with conversion of tyrosines m539 and m545 to phenylalanine (mutant 569), or truncated at lysine m391 (mutant 391) (Fig. 2A). The Y539/545F mutations were introduced to allow us to determine whether, in vivo, all STAT5 signaling originates distal to tyrosine m539 (as proposed by Hansen et al. [8]), or whether tyrosine m498 and potentially more proximal residues are required, as first proposed by Smit et al. (31). Homozygous mutant 569 or mutant 391 mice were generated by mating heterozygous mice carrying one copy of the 569 or 391 mutation, respectively. Correct homologous recombination was confirmed by restriction digest and Southern blotting, and expression of the mutant GHRs was demonstrated by Northern and Western blotting of hepatic tissue, together with sequencing of the mRNA transcript (Fig. 1B to D). The unavailability of an antibody recognizing the extracellular domain of the murine

receptor in Western blots precluded determination of the molecular size of protein produced by the 391 truncation mutant. However, radioreceptor assays confirmed normal levels of specific binding of ^{125}I -labeled bGH, i.e., $3.3\% \pm 1.1\%$ WT and $2.8\% \pm 0.8\%$ mutant 391 (mean \pm the standard error of the mean [SEM]), expressed per milligram of membrane protein ($n = 3$ samples), to the receptor in this mutant.

Signaling by mutant GHR. The main aim of the present study was to determine the effects of mutations changing the intracellular signaling of GHR on growth and metabolism. Therefore, the relative phosphorylation of main effectors of GH stimulation, such as JAK2, ERK1/2, and STAT5, was compared 15 min after mice were injected with bGH or saline. In order to observe a direct response to GH, 19-day-old mice, which have low endogenous GH secretion (2) were used. Both mutants displayed a JAK2 phosphorylation response (Fig. 2B and E) and ERK1/2 activation (Fig. 2C and F) by GH that was not significantly different from that of WT mice with similar fold induction. In contrast, mutant 569 mice exhibited a sub-

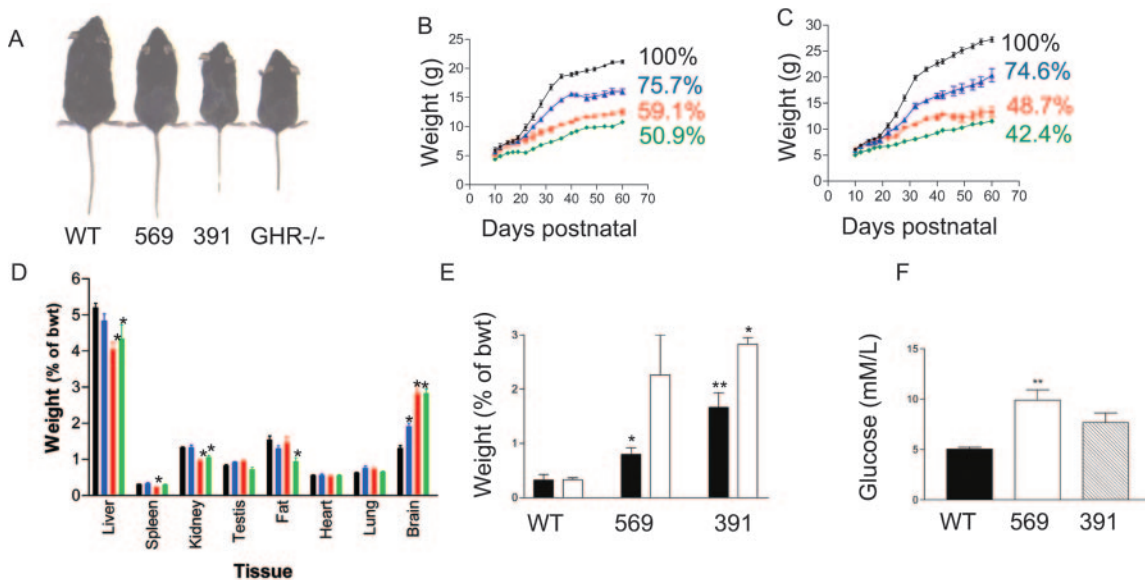


FIG. 3. Postnatal growth reduction of the GHR mutant mice. (A) Photograph of WT and mutant homozygous 60-day-old male mice. (B to D) Color coded as follows: WT (black), mutant 569 (blue), mutant 391 (red), and GHR^{-/-} (green). (B and C) Postnatal growth curves (B, females; C, males). All mice were weighed over a period of 60 days. The results are presented as mean body weight \pm the SEM ($n = 8$). Growth was significantly reduced in all mutants compared to WT ($P < 0.001$). (D) Organ weights were recorded at 60 days postnatally. The results are shown as relative to body weight and are expressed as means \pm the SEM ($n = 6$ to 8). The sizes of some organs were significantly reduced (all changes are marked with a single asterisk due to space constraints; $P < 0.01$ for all changes, except $P < 0.05$ for spleen in mutant 391 and liver in GHR^{-/-} mice). (E) Subcutaneous fat pad sizes at 4 (■) and 10 (□) months in male mice. The results are expressed relative to body weight and are means \pm the SEM ($n = 3$ to 4). **, $P < 0.01$; *, $P < 0.05$. (F) Glucose levels in 10-month-old males after a 16 h fasting ($n = 3$) and are shown as means \pm the SEM (*, $P < 0.01$).

maximal STAT5 tyrosine phosphorylation response ($29 \pm 10\%$ of WT [mean \pm the SEM; $n = 6$]), whereas no response was detectable in mutant 391 (Fig. 2D and G).

Postnatal growth rate and organ weights. Homozygous mice carrying the mutations remained phenotypically normal until ca. 3 weeks of age, after which a clear deviation in growth rates became apparent (Fig. 3), being more obvious in the mutant 391 than in mutant 569 (Fig. 3A to C). The 391 mutants grew significantly more than the GHR^{-/-} mice, which were kindly supplied by J. J. Kopchick and K. T. Coschigano (45). Heterozygotes for both mutant types also showed a significant impairment of postnatal growth and a reduction in hepatic IGF-1 transcripts, suggesting competitive inhibition of the full-length GHR at the cell surface by mutant receptor subunits, forming heterodimeric complexes (data not shown). A pronounced heterozygote effect has been reported for patients expressing cytoplasmic domain truncated mutant GHRs, which are overexpressed at the cell surface with long residence times (1).

Organ weights were measured at 60 days for mutants 569 and 391 and compared to WT and GHR^{-/-} controls. A proportional reduction in absolute organ weight was observed with severity of truncation. When the organ weight was normalized to the body weight (Fig. 3D), the spleen weight was reduced in mutant 391 ($P < 0.05$), whereas the kidney size was reduced in mutant 391 and the GHR^{-/-} control ($P < 0.01$ for both). A disproportionate reduction in liver weight was also found for mutant 391 and the GHR^{-/-} control compared to WT controls ($P < 0.01$ for mutant 391 and $P < 0.05$ for GHR^{-/-} control). On the other hand, the brain/body weight ratio was disproportionately increased in mutants 569 and 391 ($P < 0.01$

for both), as has been previously reported for the GHR^{-/-} mice. This has been attributed to the fact that brain growth is virtually complete prior to 3 weeks postnatal age, before growth hormone influences postnatal growth (16).

The GHR^{-/-} male mice showed a significant reduction in the size of the epididymal adipose pad ($P < 0.05$) in young adult animals (mice ≤ 60 days old) (Fig. 3D), but no reduction was observed in mutants 391 and 569. However, in older males (4 and 10 months), an increase in the relative weight of fat pads in all fat depots has been noted. The difference from WT mice in the amount of fat was most dramatic in the subcutaneous fat pad (Fig. 3E) and increased with age. This increased obesity was associated with substantial fasting hyperglycemia (Fig. 3F) in older mice. At the same time, no differences in fat depots or fasted glucose levels were observed in females at up to 8 months of age.

IGF-1 axis. IGF-1 is a major mediator of the growth actions of GH, so correlations between IGF-1 level and growth rates were sought. Changes in the IGF-1 axis were observed for both mutant lines (Fig. 4). The levels of hepatic *Igf1* transcripts were reduced for both mutant types (to 36% [*Igf1b* transcript] and 67% [*IGF1a*, major transcript] of WT for mutant 569 and to 9 to 11% [both transcripts] of WT for mutant 391). However, the IGF-1 level in serum was reduced further than would be indicated by hepatic transcript changes (16 to 21% of WT for mutant 569 and $< 10\%$ of WT for mutant 391 [Fig. 4B]). Ligand blotting with radiolabeled IGF-1 revealed no consistent changes in the levels of IGFBP-1, IGFBP-2, IGFBP-4, and IGFBP-5 in the sera of 42-day-old mice (Fig. 4C). However, a moderate reduction in IGFBP-3 levels was observed for mu-

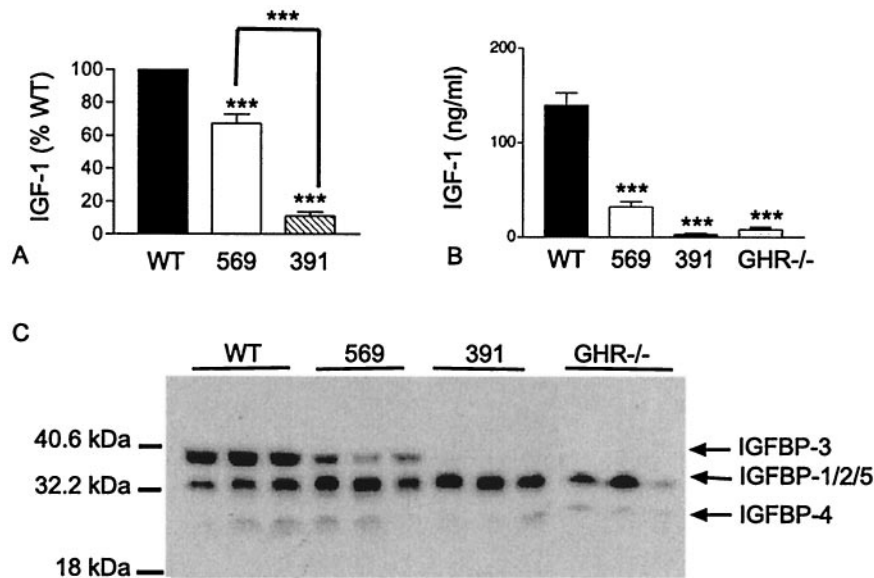


FIG. 4. IGF-1 axis in GHR mutant mice. (A) Densitometric quantification of a Northern blot analysis of the IGF-1 levels in GHR mutant mice and WT littermates. Transcripts of 0.9 to 1.2 kb were used for this analysis. The data are shown as percentages of WT and are displayed as means \pm the SEM ($n = 10$). (B) Levels of IGF-1 serum as measured by radioimmunoassay (see Materials and Methods) were significantly decreased in mutant 569, mutant 391, and GHR^{-/-} mice in comparison to WT ($P < 0.001$). The results are shown as means \pm the SEM ($n = 7$ to 11). (C) Western ligand blot profile of IGFBP levels in serum in mice at 42 days shows a significant decrease in the levels of IGFBP3 ($P < 0.001$), with no change detected in the remaining IGFBPs.

tant 569 (33 to 52% of WT), whereas a severe reduction of IGFBP-3 levels was seen with mutant 391 (6.2% of WT) and GHR^{-/-} mice (11.6% of WT). The severity of IGF-1 reduction in serum (compare Fig. 4A with Fig. 4B) suggests that additional IGF-1 degradation is taking place due to a lack of sufficient ternary ALS/IGFBP-3/IGF-1 complex to maintain a circulating IGF-1. In fact, microarray analysis (described below) showed that hepatic *Igfals* transcripts were reduced by 1.8-fold in mutant 569 and were absent in mutant 391 and GHR^{-/-} mice (see Table 1).

Because the decrease in hepatic *Igf1* transcripts and of IGF-1 in serum in the 391 mutant line was substantially greater than that reported in the STAT5a/b double-null mice (35), alterations in other hepatic factors that regulate IGF-1 production were sought. A major decrease in HNF3 β protein in the 391 mutants and a significant decrease in the 569 mutants were observed, whereas HNF1 remained unchanged (Fig. 5).

Microarray analysis of GHR knockin mice. A second aim of the present study was to relate particular signaling domains of the receptor to particular sets of GH-regulated genes. Accordingly, Affymetrix U74Av2 microarrays were used to examine differences in hepatic transcript expression between the two lines of mature mutant mice and WT littermates. GHR^{-/-} mice, without a functional GHR, were also included to determine the full extent of GH action in regulating the hepatic transcriptome (45). The average number of present calls was 35.9% so, on average, 4,483 transcripts were detected in the samples analyzed. The direction of changes in expression, in relation to a baseline of WT, was determined by MAS 5.0 software and, to be considered a significant change, was required to be at least 1.5-fold different and changed in the same direction in at least eight of nine comparisons when analyzed by using Affymetrix DMT. Changes in seven of nine compar-

isons were considered likely changes but, unless a confirmation was performed, these results were not included in the present study. This fold cutoff was selected because previously it has been reported to define regulated genes (43). This was confirmed in our experiments by analysis of *Igf1* transcripts, for which MAS 5.0 identified a 1.5-fold decrease for mutant 569, and which was shown to be significant both by Northern blot analysis and by IGF-1 immunoassay in serum (Fig. 4A and B).

Differential gene expression in mutant 569, mutant 391, and GHR^{-/-} mice compared to the WT. A set of 403 transcripts, representing 398 individual genes, which were differentially expressed across all animal groups and which met the above criteria, were identified. Twenty transcripts were common between the three receptor mutants in comparison to WT mice, with 13 unique to mutant 569, 59 unique to mutant 391, and 268 unique to the GHR^{-/-} line (Fig. 4A and Table 1). Further analysis was performed with a subset of the 398 genes that passed stringent MAS 5.0 criteria (change $P < 0.0025$ and SLR > 1 or SLR < 1) by using an analysis of variance t test with a cutoff score of $P < 0.0005$. Such a combination of criteria guarantees the lowest possible number of false positives (18, 24). Using these criteria, we have identified five genes to be regulated exclusively by m569-650 (Y539/545-F). The fold changes for these genes did not vary significantly between the mutant 569, 391, and GHR^{-/-} lines and $P > 0.0005$. There were four genes upregulated to a similar extent in all groups (*Gstt1*, *Ang*, *Papps2*, and *Serpina6*) and only one gene similarly downregulated (*Fabp5*) with at least one of the genes, *Serpina6* (corticosteroid binding globulin) known to be a direct GH target. This implies that most of the active STAT5, as well as SHP2, which binds in the m569-650 sequence, plays only a minor role in GH signaling to the genome. This upregulation of four of five genes and the fact that the majority of transcripts

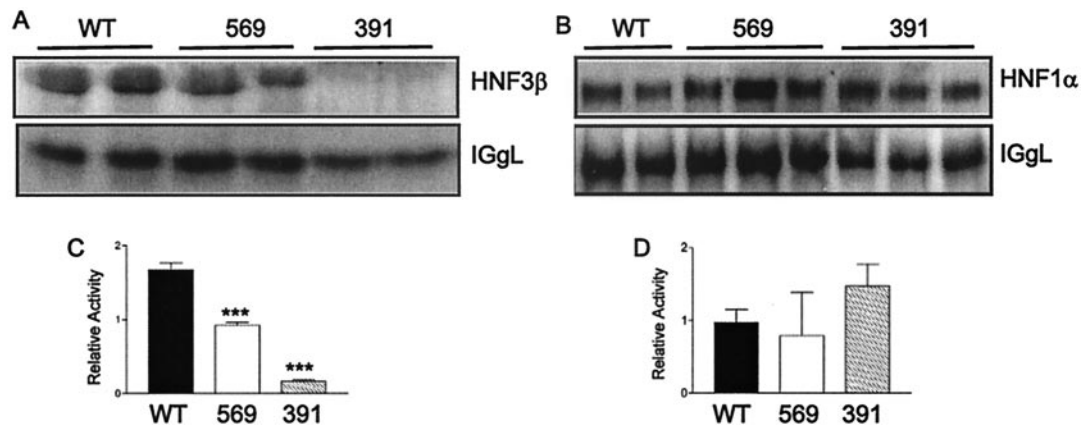


FIG. 5. Regulation of hepatic nuclear factors in GHR mutant mice. (A and B) Western blot analysis of the expression of HNF3 β (A) and HNF1 α (B) in the livers of 10-month-old mice fasted for 16 h. Both HNFs were immunoprecipitated from the liver homogenates, and immunoglobulin G light chain was used as a loading control. (C and D) Densitometric quantification of the results from panels A and B are shown as means \pm the SEM ($n = 3$). ***, $P < 0.001$.

changed in mutant 569 (Fig. 6A) were upregulated reinforces the fact that the most distal part of the receptor is important for negative modulation of GH-induced gene expression. Furthermore, the set of 20 common genes (Table 1), which were regulated concordantly in the mutant 569, mutant 391, and GHR $^{-/-}$ mice, was identified. These genes can be reasonably assigned as STAT5-regulated genes since they included known STAT5-regulated genes such as *Igf1*, *Igfals*, *Socs2*, P450 cytochrome, *Cyp2b9*, and some metabolic enzymes. Eleven of these

TABLE 1. Genes regulated concordantly in mutant 569, mutant 391, and GHR $^{-/-}$ mice

| Gene | Fold change ^a | | | Known regulation by GH ^b |
|------------------------------------------------|--------------------------|---------------|------------------|-------------------------------------|
| | Mutant 569/WT | Mutant 391/WT | GHR $^{-/-}$ /WT | |
| Genes upregulated in all three groups | | | | |
| <i>Ang</i> | 2.1 | 3.3 | 2.8 | |
| <i>Cyp2b9</i> | 5.2 | 10.9 | 15.3 | |
| <i>Cyp4a10</i> | 2.1 | 2.6 | 2.0 | |
| <i>Cyp17a1</i> | 3.4 | 4.0 | 2.5 | |
| <i>Gsta4</i> | 2.2 | 2.5 | 4.7 | |
| <i>Gstt1</i> | 1.6 | 2.2 | 1.6 | |
| <i>Hao3</i> | 3.8 | 11.7 | 9.4 | + |
| <i>Papps2</i> | 1.6 | 3.0 | 2.3 | |
| <i>Serpina6</i> | 2.0 | 2.6 | 3.1 | + |
| <i>Sih2</i> | >10* | >10* | >10* | + |
| <i>Sultn</i> | 1.8 | 2.4 | 1.9 | |
| Genes downregulated in all three groups | | | | |
| <i>1100001G20</i> | -3.0 | <-10† | <-10† | |
| <i>Comt</i> | -1.9 | -4.2 | -2.8 | + |
| <i>Csad</i> | -2.6 | -6.2 | -6.1 | |
| <i>Egfr 101841_at</i> | -2.5 | <-10† | <-10† | + |
| <i>Egfr 101842_g_at</i> | <-10† | <-10† | <-10† | + |
| <i>Fabp5</i> | -3.3 | -4.1 | -4.6 | |
| <i>Hsd3b5</i> | -24.7 | <-10† | <-10† | |
| <i>Igfals</i> | -1.8 | <-10† | <-10† | + |
| <i>Orn1</i> | -1.8 | -5.5 | -2.7 | + |

^a Values indicate changes with WT values as a baseline. *, transcript absent in WT mice; †, transcript absent in mutant mice as determined by MAS 5.0 software.

^b +, regulation detected.

were upregulated (e.g., *Sih2*, *Hao3*, and *Ang*), and nine were downregulated (e.g., *Igfals*, *Igf1*, *Egfr*, and *Comt*); among these genes at least seven are currently known to be direct targets of GH-induced signaling. Increased downregulation of the *Igf1* transcript in the 391 mutant suggests that the residual 30% of active STAT5 plays an important role in regulation of *Igf1* (and presumably many other) transcripts, and *Igf1* mRNA levels are critically dependent on STAT5 both in vitro and clinically, based on loss-of-function studies (13, 41).

The analysis of the 121 transcripts altered in the mutant 391 showed that the majority of transcripts were not affected in mutant 569 and that 41 of them were not different from the GHR $^{-/-}$ mice (e.g., *Apcs*, *Es31*, *Cdkn1c*, *Ndufb8*, *Iigp-pending*, *Lifr*, and *Mug-ps1*) (Table 2 and Fig. 6A). The expression of these genes, as well as genes regulated preferentially in mutant 391 mice (*Hsd3b3* and *Hsd3b6*), may be directed by the signaling proteins docking at all or some of the three tyrosines that were removed by the 391 mutation (residues m402, m465, and m498), which would include residual STAT5. The promoters of these genes may be either particularly sensitive to STAT5 or dependent on other signaling pathways within the m391-569 sequence. Such pathways include the Ca²⁺ signaling element between m465 and m517 and potentially other uncharacterized pathways.

The largest number of altered transcripts was observed for GHR $^{-/-}$ mice ($n = 330$), providing a striking contrast to the 121 regulated transcripts for mutant 391 mice despite a very similar extent of growth retardation. These genes, presumably directly regulated by JAK2 and associated ERK1/2 and PI 3-kinase pathways, as well as negatively by SOCS proteins, include many metabolic genes, as well as genes regulating signaling, proliferation, translation, and transporter proteins. Such genes represent the core functions of the hepatocyte and are most likely regulated by elements common to all cytokine and tyrosine kinase receptors. Some of these genes have been shown to be directly regulated by GH (e.g., *Igf1*, *Socs2*, or *Comt*) (36) (Tables 1 and 2); some are likely to be regulated by transcription factors induced by GH signaling. In fact, the important differences between the GHR $^{-/-}$ mice and the mu-

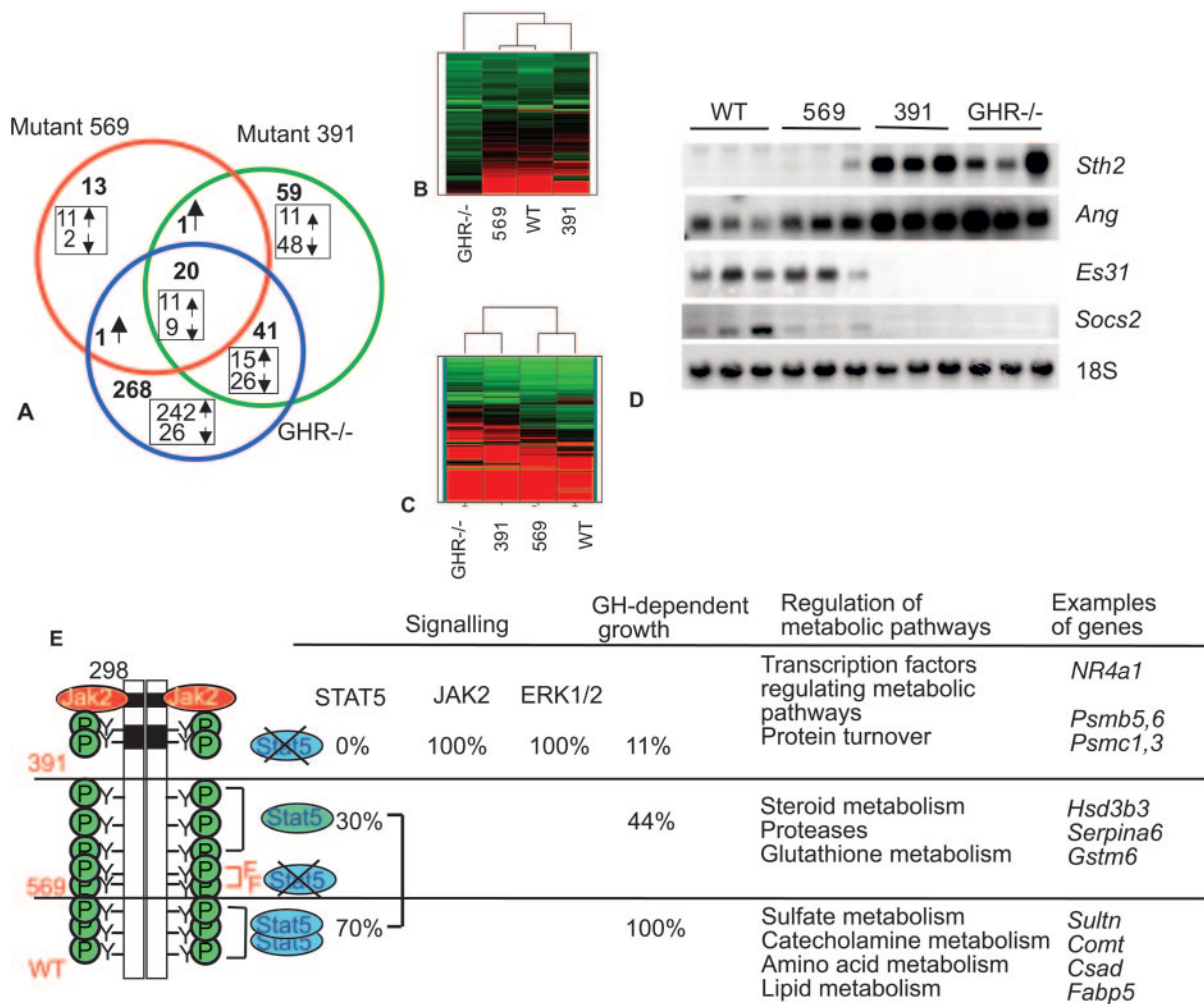


FIG. 6. Global analysis of the GHR mutant mice by using microarrays. (A) Venn diagram showing the number of genes differentially expressed in the three knockin lines compared to WT mice and the number of genes up- and downregulated in each group. Genes expressed in common between the mutants are indicated by overlaps of the circles. (B and C) Hierarchical clustering was performed with DecisionSite 7.2 software (functional genomics module). (B) Mutant 569 is most similar in its pattern of gene expression to the WT, and mutant 391 is similar to these two groups and to GHR^{-/-} mice cluster separately. This clustering was generated by using the average signal (*n* = 3) for all probe sets from the arrays, with exclusion of genes absent in all groups. (C) Metabolically, mutant 569 is most similar to WT mice in its gene expression pattern, whereas mutant 391 is most similar to GHR^{-/-} mice. This clustering was performed by using average signal (*n* = 3) for probe sets representing genes encoding proteins involved in metabolism. (D) Northern blot confirmation of microarray results. Total RNA from the 42-day-old mice was run on a 1% denaturing gel, blotted onto a nylon membrane, and probed with probes targeting the same region of the gene as the Affymetrix probes. The blot was then reprobed with 18S oligomer probe to confirm loading. (E) Changes in signaling and GH-dependent growth in GHR^{-/-} mice. A summary of the results shows that in WT mice 100% signaling through all major pathways contributes to 100% of GH-dependent growth, whereas in mutant 569 the loss of 70% of STAT5 signaling results in the loss of 66% of GH-dependent growth, and the absence of active STAT5 pathway in mutant 391 is not adequate to reduce GH-dependent growth to zero; these mice retain 11% of this growth. Metabolic pathways identified by GO analysis and examples of genes belonging to each category that were differentially expressed are shown (<http://research.imb.uq.edu.au/~mwaters/ghr/>).

tant mice were the upregulation of transcription and elongation factors (e.g., *Nr4a1*, *Bcl6*, *Egr-1*, *Dbp*, and *Tcea3*) and the upregulation of translational factors (e.g., *Sui1-rs1*, *Eef1d*, and *Ict1*), none of which was significantly changed in mutants 569 and 391. This suggests that in GHR^{-/-} mice a number of transcripts regulated by these factors would be expressed at a higher level than in WT mice. This could account for a substantial proportion of the genes uniquely increased in the GHR^{-/-} mice compared to the mutants and WT (e.g., *Rgs16*, *Cops3*, *Ppap2a*, *Gphn*, and *Gkap42-pending*).

Classification of the regulated genes by GO highlights the

main differences and similarities between the four lines of mice (Table 3 and <http://research.imb.uq.edu.au/~mwaters/ghr/>). We have explored the relationships between cell lines by using hierarchical clustering based on all transcripts (Fig. 6B) or based on metabolic genes (Fig. 6C). Mutant 569 and WT were most similar in both analyses, and although mutant 391 was similar to mutant 569 and WT based on overall gene expression, mutant 391 appeared to be more similar to GHR^{-/-} mice in relation to metabolic genes. Both of these observations support our phenotypic findings (Fig. 2 and 3), in that mutant 391 retains JAK2 and ERK1/2 signaling and thus

TABLE 2. Genes that are specific to the signaling domains of the ICD of the GHR

| Gene | | Change ^a | | | | | | Known GH-regulated genes ^b |
|----------------------------------------------------------------------------------------------|----------------------|---------------------|------|------------|----------------|------------|----------------|---------------------------------------|
| AFFY ID ^d | Name | GHR ^{-/-} | | Mutant 391 | | Mutant 569 | | |
| | | Fold | Type | Fold | Type | Fold | Type | |
| Genes not changed in mutant 569 | | | | | | | | |
| 95620_at | <i>2310016E22Rik</i> | 2.3 | I | 2.0 | I | 1.4 | NC | |
| 95471_at | <i>Cdkn1c</i> | 2.1 | I | 2.6 | I | 1.1 | NC | |
| 93581_at | <i>Ndufb8</i> | 2.7 | I | 2.4 | I | 1.3 | NC | |
| 104072_at | <i>Apcs</i> | -2.7 | D | -2.8 | D | -1.3 | NC | |
| 99941_at | <i>Es31</i> | <-10* | D | <-10* | D | -1.4 | NC | |
| 103963_f_at | <i>ligp-pending</i> | -3.8 | D | -3.0 | D | 1.1 | NC | |
| 96938_at | <i>Keg1</i> | <-10* | D | <-10* | D | -1.5 | NC | |
| 97680_at | <i>Mug-ps1</i> | -2.3 | D | -2.5 | D | -1.2 | NC | |
| 101910_f_at | <i>Mup1</i> | -4.2 | D | -3.8 | D | -1.3 | NC | + |
| 161815_f_at | <i>Mup1</i> | -5.0 | D | -5.9 | D | -1.3 | NC | + |
| 102096_f_at | <i>Mup1</i> | -5.9 | D | -6.5 | D | -1.4 | NC | + |
| 101566_f_at | <i>Mup1</i> | -3.9 | D | -2.6 | D | -1.1 | NC | + |
| 101909_f_at | <i>Mup3</i> | -4.0 | D | -3.7 | D | -1.3 | NC | |
| 101682_f_at | <i>Mup4</i> | -4.3 | D | -4.3 | D | -1.3 | NC | |
| 101635_f_at | <i>Mup5</i> | -4.0 | D | -3.5 | D | -1.3 | NC | |
| Genes changed in mutant 569 and not different between mutant 391 and GHR ^{-/-} mice | | | | | | | | |
| 95546_g_at | <i>Igf-1</i> | <-10* | D | <-10* | D | -1.5 | D ^c | + |
| 99475_at | <i>Socs2</i> | <-10* | D | <-10* | D | -1.2 | D ^c | + |
| Genes not changed in mutant 569 and mutant 391 | | | | | | | | |
| 93986_at | <i>2410003A14Rik</i> | 2.1 | I | 1.1 | NC | 1.2 | NC | |
| 94844_at | <i>2810465O16Rik</i> | -2.8 | D | -1.1 | NC | -1.2 | NC | |
| 97201_s_at | <i>2900002J19Rik</i> | 2.0 | I | 1.3 | NC | 0.0 | NC | |
| 102804_at | <i>Ceacam1</i> | -2.3 | D | -1.3 | NC | -1.1 | NC | |
| 160711_at | <i>Decr1</i> | 2.4 | I | 1.6 | NC | 1.2 | NC | + |
| 92571_at | <i>Hspa4</i> | 2.0 | I | -1.1 | NC | -1.1 | NC | + |
| 162006_r_at | <i>Immt</i> | -4.2 | D | -1.3 | NC | -1.1 | NC | |
| 94056_at | <i>Scd1</i> | -2.4 | D | -1.3 | NC | 0.0 | NC | + |
| 93348_at | <i>Timm22</i> | 2.0 | I | -1.3 | NC | 1.3 | NC | |
| Genes gradually changing in mutant 569, mutant 391, and GHR ^{-/-} mice | | | | | | | | |
| 99669_at | <i>Lgals1</i> | 3.2 | I | 1.9 | NC | -1.1 | NC | |
| 161161_r_at | <i>Nme1</i> | -5.3 | D | -1.9 | NC | -1.2 | NC | |
| 100437_g_at | <i>Orm1</i> | -2.7 | D | -5.5 | D | -1.7 | D | + |
| 95030_at | <i>Prlr</i> | -4.9 | D | -2.3 | D | -1.7 | D ^c | + |
| 99591_i_at | <i>Rdh11</i> | -3.3 | D | -2.0 | D | -1.6 | NC | |
| 103465_f_at | <i>Saa2</i> | 3.6 | I | 1.6 | NC | 1.3 | NC | |
| 93084_at | <i>Slc25a4</i> | 3.1 | I | 1.4 | NC | 1.1 | NC | |
| 161257_r_at | <i>Snx17</i> | -4.4 | D | -2.6 | D ^c | -1.7 | NC | |
| Genes changed in mutant 391 only | | | | | | | | |
| 98401_at | <i>Hsd3b3</i> | -1.1 | NC | -3.1 | D | -1.1 | NC | |
| 102729_f_at | <i>Hsd3b6</i> | -1.3 | NC | -3.0 | D | -1.2 | NC | |

^a Values are changes with WT values as a baseline. Change types were identified by MAS 5.0 software in comparison to the WT base file: NC, no change; I, increase; D, decrease. *, transcript absent in mutant mice as determined by MAS 5.0 software.

^b +, regulation detected.

^c Decrease or increase in seven of nine comparisons (indicating a likely change).

^d AFFY ID, Affymetrix identification number.

should be more similar to mutant 569 and WT than to GHR^{-/-} mice. On the other hand, the levels of STAT5-dependent transcripts such as *Igf-1* and *Socs-2* in mutant 391 were more similar to GHR^{-/-} mice (Table 2 and Fig. 6D). Mutant 391 and GHR^{-/-} also shared similar alterations in transcripts encoding a number of transporters, signaling molecules, and cytochromes, as well as electron transport proteins. This GO

analysis supports the view that we have delineated functional domains within the cytoplasmic signaling unit of the GHR in vivo.

DISCUSSION

A main aim of this study was to define the region(s) of the GHR cytoplasmic domain responsible for enhancing postnatal

TABLE 3. Simplified gene ontology classification of genes differentially expressed in three transgenic lines in comparison to the WT

| Type or function | No. of genes | | |
|--------------------------------------|--------------|------------|----------------------------|
| | Mutant 569 | Mutant 391 | GHR ^{-/-} control |
| Metabolism | 12 | 26 | 60 |
| Cytochrome/electron transport | 5 | 12 | 22 |
| Glutathione/antioxidant | 2 | 8 | 10 |
| Transporters | 1 | 16 | 20 |
| Proliferation/differentiation/growth | 2 | 10 | 30 |
| Cell-to-cell interactions | 0 | 1 | 5 |
| Transcription/translation | 0 | 0 | 23 |
| Signaling | 1 | 13 | 28 |
| Protein processing | 4 | 18 | 17 |
| Chaperones | 1 | 1 | 7 |
| Ribosomal proteins | 0 | 1 | 17 |
| Unclassified | 6 | 15 | 91 |
| Total | 35 | 121 | 330 |

growth, since no cases of GH insensitivity had been reported for the signaling domain other than those involving the JAK2 binding box 1 sequence. The approach used here allows us to conclude that the distal 80 residues and the tyrosines previously thought to be responsible for all or most of the STAT5 generation account for 70% of STAT5 generation and 44% of the GH-responsive postnatal growth in the male (30) (Fig. 6E). The remaining 30% of STAT5 signaling appears adequate to retain relatively normal gene expression, even of genes known to be STAT5 responsive. This includes the main *Igf1* transcript, which was decreased by <33%. The overall correlation between STAT5 activation and *Igf1* transcript level is concordant with recent studies implicating STAT5 in the generation of IGF-1 (41). Surprisingly, the modest decrease in *Igf1* transcripts in the 569 line was associated with a substantial drop in IGF-1 in serum of ca. 80%, which appears to be necessary to achieve major growth retardation. It is likely that the level of free IGF-1 is higher in the 569 line owing to a decreased expression of IGFBP3 and IGF-ALS, which are strongly regulated by the terminal 80 residues. Because the STAT5a/b-null mice do not display the severity of growth phenotype and IGF-1 loss seen with the 391 line (which lacks the ability to generate STAT5a/b), we looked for other hepatic transcription factors that regulate IGF-1 and which are associated with the 391-to-569 sequence. Both HNF1 α and HNF3 β have been implicated in transactivation of the IGF-1 gene promoter (20, 21). Although HNF1 α expression was not altered in the 391 or 569 mutant lines, HNF3 β expression was markedly decreased in the 391 line but was also significantly reduced in the 569 line (Fig. 5). This provides an indication, for the first time, that GH may regulate hepatic IGF-1 production by a combination of STAT5a/b and HNF3 β , generated from the distal part of the GH receptor signaling domain. However, the interrelations of the hepatic nuclear factors are complex (26), and HNF3 β is induced by HNF6, which is itself under GH control via STAT5b and HNF4, the latter being rapidly and directly activated by GH in a manner which is thought to involve direct tyrosine phosphorylation (14), either of HNF4 or of its inhibitory regulator FKHR (10). Loss of STAT5 activation could

explain the significant reduction of HNF3 β seen in the 569 mice, with the severe decrease in the 391 being a result of loss of both STAT5b and receptor-dependent HNF4 activation. This severe loss is unlikely to involve the other major regulator of HNF3 β expression, C/EBP β (27), since this is activated by the ERK pathway (23), which is not affected in the 391 mutant line.

It is significant that the loss of all STAT5 signaling (391 line) is associated with a growth retardation almost as severe as receptor deletion, whereas ERK1/2 signaling is not affected. It can be concluded that non-STAT5/JAK2 signaling, including ERK and STAT3 signaling, can alone account for only ca. 10% of GH-responsive postnatal growth. This contrasts with a similar targeted knockin study with the EPO receptor, where removal of all cytoplasmic tyrosine residues resulted in only a minor effect on erythropoiesis (44). The residual 10% of GH-responsive postnatal growth even in the absence of detectable STAT5 activation and IGF-1 in serum in mutant 391 may represent the IGF-1-independent, GH-dependent element in postnatal growth (14%) identified by Lupu et al. (16) based on IGF-1^{-/-} and GHR^{-/-} crosses. In that study, IGF-1 receptor-dependent postnatal growth amounted to 70% of total postnatal growth, with 17% of postnatal growth being independent of either GH or IGF-1 (16). This GH-dependent, but IGF-1-independent growth may correspond to that seen in myeloid cells stably expressing 351 truncated GHR, which proliferate normally in response to GH (39). It is also of interest that the 391 mutant, lacking ability to generate STAT5a/b, did not show sexual dimorphism in growth, as was also observed in the STAT5b^{-/-} mice (35). This correlates with an inability to express the male-specific MUP transcripts and protein in the 391 line, as well as feminization of its cytochrome P450 profile in the liver.

Our in vivo finding that ERK activation is normal with the 391 truncation is in contrast to the findings of some in vitro studies (38) but not others (3, 33). A second in vitro conclusion that was not verified in vivo is the lack of involvement of tyrosine m498 and proximal tyrosine in the generation of activated STAT5 (8). In support of this, other in vitro studies (32) have proposed that tyrosines m498 and m545 are responsible for most of the STAT5 activation. As is evident here, tyrosines m401, m447, and m498 (most likely tyrosine m498 [30]) can generate ca. 30% of active STAT5 in the liver. The lack of ability of the 391 truncated mutant to generate STAT5 eliminates a role for tyrosines m333 and m338 in generating active hepatic STAT5.

The present study has used the novel approach of combining transcript analysis by microarray with the creation of mice bearing targeted mutations within the cytoplasmic sequence of the GH receptor in order to define the role of signaling domains within the receptor. We have been able to define a limited set of 35 hepatic transcripts (5 exclusively) which are regulated by the carboxy-terminal 80 residues, and the two adjacent tyrosines (Fig. 6A). This domain generates the majority of active STAT5, and this is likely to be the instrumental agent in regulating these mainly metabolic genes. Accordingly, some of the P450 cytochromes that are known STAT5a targets, as shown by their increase in the STAT5a^{-/-} mice, had their expression increased by deletion of this region (22). Microar-

ray analysis of STAT5a/b^{-/-} double-mutant mice should allow further definition of these regulated genes.

Despite the major involvement of residues m391 to m650 in regulating growth, the loss of the remaining receptor signaling results in a substantially greater number of altered transcripts ($n = 330$, compared to 121 for the mutant 391). The majority of transcripts changed in mutant 391 are downregulated in contrast to GHR^{-/-} mice (Fig. 6A). This observation can be explained by the presence of binding sites in this truncated mutant, for negative regulators such as SOCS proteins, whereas all repression normally provided by GH signaling is lost in GHR^{-/-} mice. In addition, these changes are accompanied in GHR^{-/-} mice by upregulation of a number of important transcription factors (e.g., *Nr4a*, *Bcl6*, *Dbp*, and *Egr-1*), as well as translational regulators.

The present study has provided substantial new data on the physiological roles of GH in hepatic function, since large-scale microarrays have not previously been applied to GHR gene-disrupted mice. Indeed, the only microarray study using Clontech Atlas gene arrays (with 1,176 genes) on the GHR^{-/-} mice identified only 10 regulated transcripts (17), with 6 of them confirmed in the present study. Several patterns emerging from the transcriptome analysis are clearest in the GHR^{-/-} mice. Transcripts related to protein synthesis and RNA metabolism are increased, whereas a number of transcripts encoding the serine protease inhibitor family were decreased. This could potentially decrease protein turnover and activation and lead to abnormal accumulation and/or actions of proteases. The changes observed in transcripts encoding metabolic enzymes, for example, in lipid and cholesterol metabolism (*Scd1*, *Decri1*, *Echl1*, and *Acaa1*) confirm a previous study showing GH regulation (36). Changes in genes involved in cholesterol metabolism involved not only genes necessary for its synthesis and cellular uptake but also for cholesterol conversion to bile acids (*Csad*). The latter was highly decreased, which can be expected to elevate the hepatic cholesterol levels. The changes in cholesterol availability would also affect steroid metabolism, and there were changes in transcripts encoding genes regulating this pathway. Transcript for one of the enzymes (*Hsd3b5*) was reduced in all mutants; however, in mutant 391 five other genes of this family were decreased. A number of transcripts encoding sugar-metabolizing enzymes (e.g., *G6pc* and *Pfkfb1*) were increased in the GHR^{-/-} mice, with mild changes in mutant 391 and no changes in mutant 569. One of the important changes observed was an increase in transcripts encoding proteins of the beta-oxidation (*Acacl1*, *Hao3*, and 1300002P22 Rik), electron transport chain (family of NADH dehydrogenases and cytochrome oxidases), and trichloroacetic acid cycle (*Idh3g* and *Suclg1*) would indicate higher energy production in GHR^{-/-} mice. At least some of these changes would account for many of the phenotypes observed in GH-deficient patients and animals. However, the finding of obesity in both lines in later life does not correlate with the observed changes in hepatic lipid metabolism. The answer in this case is likely to be in the adipose tissue itself. GH-deficient *lit/lit* mice exhibit obesity in maturity, as did the older mutant mice in the present study. A likely cause of this is the deficiency of STAT5a, which is required for GH-dependent lipolysis in adipose tissue (6). There may also be a contribution to lipogenesis from the continuing drive to the distal receptor domain from elevated GH

levels in plasma resulting from the lowered levels of IGF-1 in plasma.

An interesting finding in the young adult mice was the identification of a number of transcripts known to be important in regulating insulin sensitivity. These include the fatty acid-binding proteins 2 and 5, lipin 2, insulin-degrading enzyme, cortisol-binding globulin (*Serpina6*), and the induced in fatty liver dystrophy 2 transcript (*Iffd2*). Increased insulin sensitivity and decreased IGF-1 and insulin levels found in long-lived GHR^{-/-} mice are concordant with these findings (4), although the elevated blood glucose in older animals (associated with obesity) would argue against this in the long term. Interestingly, 14 transcripts associated with life span extension in *Caenorhabditis elegans* are similarly regulated in the GHR^{-/-} mice, raising the possibility that the life extension is not related to insulin. It will be important to determine whether mutant 569 with lowered IGF1 and mild growth retardation displays longevity similar to the heterozygous IGF1R^{+/-} mouse (11), or if this is only seen with extreme suppression of IGF-1, as seen in the mutant 391, or correlates with loss of GH stimulated PI 3-kinase and ERK1/2 activity, as seen in the GHR^{-/-} mice.

The present study has described the role of the various parts of the cytoplasmic domain of GHR in generating growth signal, indicated significant changes in metabolism associated with mutations of GHR (Fig. 6E), and provided evidence for novel roles of GH. In particular, the changes observed in GHR^{-/-} mice indicated a role of GH in regulating mRNAs for transcription factors critical in promoting inflammation (*Pparγ*, *Nr4a1*, and *Bcl6*) and transcripts for complement genes, for *Rgs16* and *Zap 70*, and for interleukin-1 receptor antagonist, which together could account for the mortality observed when GH treatment is given to critically ill patients. In many cases the known roles of GH are more extensive than previously thought as, for example, in the regulation of antioxidant and glutathione metabolism, serum proteins, Serpin genes, RNA/DNA-binding proteins, chaperones, and ribosomal proteins, the latter presumably increasing translation efficiency. The results presented here also show that the GH-regulated metabolic functions can be successfully studied in our GHR mutant animals. Such studies will, however, require a physiological stress (e.g., induction of diabetes or use of specific diet) to determine how various enzymes and other proteins are regulated by remaining GH signaling. Further defining of the in vivo signaling pathways responsible for the regulation of expression of GH-induced genes will be facilitated by other targeted mutations to the cytoplasmic domain of the GH receptor.

ACKNOWLEDGMENTS

We appreciate the generosity of J. J. Kopchick and K. T. Coschigano for supplying us with the GH receptor-deleted mice used in this study. We thank Paul Addison and Terry Daly for excellent technical assistance. We thank Melissa Little and Christine Wells for creating the 129X1/SvJ ES cell line (C1368) and allowing us to use it.

This study was supported by the National Health and Medical Research Council of Australia.

REFERENCES

1. Ayling, R. M., R. Ross, P. Townner, S. Von Laue, J. Finidori, S. Moutoussamy, C. R. Buchanan, P. E. Clayton, and M. R. Norman. 1997. A dominant-

- negative mutation of the growth hormone receptor causes familial short stature. *Nat. Genet.* **16**:13–14.
2. **Choi, H. K., and D. J. Waxman.** 2000. Plasma growth hormone pulse activation of hepatic JAK-STAT5 signaling: developmental regulation and role in male-specific liver gene expression. *Endocrinology* **141**:3245–3255.
 3. **Colosi, P., K. Wong, S. R. Leong, and W. I. Wood.** 1993. Mutational analysis of the intracellular domain of the human growth hormone receptor. *J. Biol. Chem.* **268**:12617–12623.
 4. **Coschigano, K. T., D. Clemmons, L. L. Bellush, and J. J. Kopchick.** 2000. Assessment of growth parameters and life span of GHR/BP gene-disrupted mice. *Endocrinology* **141**:2608–2613.
 5. **Davey, H. W., T. Xie, M. J. McLachlan, R. J. Wilkins, D. J. Waxman, and D. R. Grattan.** 2001. STAT5b is required for GH-induced liver IGF-I gene expression. *Endocrinology* **142**:3836–3841.
 6. **Fain, J. N., J. H. Ihle, and S. W. Bahouth.** 1999. Stimulation of lipolysis but not of leptin release by growth hormone is abolished in adipose tissue from Stat5a and b knockout mice. *Biochem. Biophys. Res. Commun.* **263**:201–205.
 7. **Gu, H., Y. R. Zou, and K. Rajewsky.** 1993. Independent control of immunoglobulin switch recombination at individual switch regions evidenced through Cre-loxP-mediated gene targeting. *Cell* **73**:1155–1164.
 8. **Hansen, L. H., X. Wang, J. J. Kopchick, P. Bouchelouche, J. H. Nielsen, E. D. Galsgaard, and N. Billestrup.** 1996. Identification of tyrosine residues in the intracellular domain of the growth hormone receptor required for transcriptional signaling and Stat5 activation. *J. Biol. Chem.* **271**:12669–12673.
 9. **Herrington, J., and C. Carter-Su.** 2001. Signaling pathways activated by the growth hormone receptor. *Trends Endocrinol. Metab.* **12**:252–257.
 10. **Hirota, K., H. Daitoku, H. Matsuzaki, N. Araya, K. Yamagata, S. Asada, T. Sugaya, and A. Fukamizu.** 2003. Hepatocyte nuclear factor-4 is a novel downstream target of insulin via FKHR as a signal-regulated transcriptional inhibitor. *J. Biol. Chem.* **278**:13056–13060.
 11. **Holzenberger, M., J. Dupont, B. Ducos, P. Leneuve, A. Geloën, P. C. Even, P. Cervera, and Y. Le Bouc.** 2003. IGF-1 receptor regulates lifespan and resistance to oxidative stress in mice. *Nature* **421**:182–187.
 12. **Hossenlopp, P., D. Seurin, B. Segovia-Quinson, S. Hardouin, and M. Binoux.** 1986. Analysis of serum insulin-like growth factor binding proteins using Western blotting: use of the method for titration of the binding proteins and competitive binding studies. *Anal. Biochem.* **154**:138–143.
 13. **Kofoed, E. M., V. Hwa, B. Little, K. A. Woods, C. K. Buckway, J. Tsubaki, K. L. Pratt, L. Bezrodnik, H. Jasper, A. Tepper, J. J. Heinrich, and R. G. Rosenfeld.** 2003. Growth hormone insensitivity associated with a STAT5b mutation. *N. Engl. J. Med.* **349**:1139–1147.
 14. **Lahuna, O., M. Rastegar, D. Maiter, J. P. Thissen, F. P. Lemaigre, and G. G. Rousseau.** 2000. Involvement of STAT5 (signal transducer and activator of transcription 5) and HNF-4 (hepatocyte nuclear factor 4) in the transcriptional control of the *hmf6* gene by growth hormone. *Mol. Endocrinol.* **14**:285–294.
 15. **Lobie, P. E., T. J. Wood, C. M. Chen, M. J. Waters, and G. Norstedt.** 1994. Nuclear translocation and anchorage of the growth hormone receptor. *J. Biol. Chem.* **269**:31735–31746.
 16. **Lupu, F., J. D. Terwilliger, K. Lee, G. V. Segre, and A. Efstratiadis.** 2001. Roles of growth hormone and insulin-like growth factor 1 in mouse postnatal growth. *Dev. Biol.* **229**:141–162.
 17. **Miller, R. A., Y. Chang, A. T. Galecki, K. Al-Regaiey, J. J. Kopchick, and A. Bartke.** 2002. Gene expression patterns in calorically restricted mice: partial overlap with long-lived mutant mice. *Mol. Endocrinol.* **16**:2657–2666.
 18. **Miller, R. A., A. Galecki, and R. J. Shmookler-Reis.** 2001. Interpretation, design, and analysis of gene array expression. *J. Gerontol. Ser. A Biol. Sci. Med. Sci.* **56**:B52–B57.
 19. **Milward, A., L. Metherell, M. Maamra, M. J. Barahona, I. R. Wilkinson, C. Camacho-Hubner, M. O. Savage, C. M. Bidlingmaier, A. J. Clark, R. J. Ross, and S. M. Webb.** 2004. Growth hormone (GH) insensitivity syndrome due to a GH receptor truncated after Box1, resulting in isolated failure of STAT 5 signal transduction. *J. Clin. Endocrinol. Metab.* **89**:1259–1266.
 20. **Nolten, L. A., P. H. Steenbergh, and J. S. Sussenbach.** 1995. Hepatocyte nuclear factor 1 alpha activates promoter 1 of the human insulin-like growth factor I gene via two distinct binding sites. *Mol. Endocrinol.* **9**:1488–1499.
 21. **Nolten, L. A., P. H. Steenbergh, and J. S. Sussenbach.** 1996. The hepatocyte nuclear factor 3beta stimulates the transcription of the human insulin-like growth factor I gene in a direct and indirect manner. *J. Biol. Chem.* **271**:31846–31854.
 22. **Park, S. H., X. Liu, L. Hennighausen, H. W. Davey, and D. J. Waxman.** 1999. Distinctive roles of STAT5a and STAT5b in sexual dimorphism of hepatic P450 gene expression: impact of STAT5a gene disruption. *J. Biol. Chem.* **274**:7421–7430.
 23. **Piwien Pilipuk, G., M. D. Galigniana, and J. Schwartz.** 2003. Subnuclear localization of C/EBP β is regulated by growth hormone and dependent on MAPK. *J. Biol. Chem.* **278**:35668–35677.
 24. **Rajagopalan, D.** 2003. A comparison of statistical methods for analysis of high-density oligonucleotide array data. *Bioinformatics* **19**:1469–1476.
 25. **Ram, P. A., and D. J. Waxman.** 1999. SOCS/CIS protein inhibition of growth hormone-stimulated STAT5 signaling by multiple mechanisms. *J. Biol. Chem.* **274**:35553–35561.
 26. **Rastegar, M., F. P. Lemaigre, and G. G. Rousseau.** 2000. Control of gene expression by growth hormone in liver: key role of a network of transcription factors. *Mol. Cell Endocrinol.* **164**:1–4.
 27. **Rausa, F., U. Samadani, H. Ye, L. Lim, C. F. Fletcher, N. A. Jenkins, N. G. Copeland, and R. H. Costa.** 1997. The cut-homeodomain transcriptional activator HNF-6 is coexpressed with its target gene HNF-3 β in the developing murine liver and pancreas. *Dev. Biol.* **192**:228–246.
 28. **Sambrook, J., E. F. Fritsch, and T. Maniatis.** 1989. *Molecular cloning: a laboratory manual*, 2nd ed. Cold Spring Harbor Laboratory Press, Cold Spring Harbor, N.Y.
 29. **Schwenk, F., U. Baron, and K. Rajewsky.** 1995. A cre-transgenic mouse strain for the ubiquitous deletion of loxP-flanked gene segments including deletion in germ cells. *Nucleic Acids Res.* **23**:5080–5081.
 30. **Smit, L. S., D. J. Meyer, L. S. Argetsinger, J. Schwartz, and C. Carter-Su.** 1997. Molecular events in growth hormone-receptor interaction and signaling, p. 445–480. *In* J. L. Kostyo and H. M. Goodman (ed.), *Handbook of physiology*, vol. 5. Oxford University Press, Oxford, United Kingdom.
 31. **Smit, L. S., D. J. Meyer, N. Billestrup, G. Norstedt, J. Schwartz, and C. Carter-Su.** 1996. The role of the growth hormone (GH) receptor and JAK1 and JAK2 kinases in the activation of Stats 1, 3, and 5 by GH. *Mol. Endocrinol.* **10**:519–533.
 32. **Sotiropoulos, A., S. Moutoussamy, F. Renaudie, M. Clauss, C. Kayser, F. Gouilleux, P. A. Kelly, and J. Finidori.** 1996. Differential activation of Stat3 and Stat5 by distinct regions of the growth hormone receptor. *Mol. Endocrinol.* **10**:998–1009.
 33. **Sotiropoulos, A., M. Perrot-Appianat, H. Dinerstein, A. Pallier, M. C. Postel-Vinay, J. Finidori, and P. A. Kelly.** 1994. Distinct cytoplasmic regions of the growth hormone receptor are required for activation of JAK2, mitogen-activated protein kinase, and transcription. *Endocrinology* **135**:1292–1298.
 34. **Tannenbaum, G. S., H. K. Choi, W. Gurd, and D. J. Waxman.** 2001. Temporal relationship between the sexually dimorphic spontaneous GH secretory profiles and hepatic STAT5 activity. *Endocrinology* **142**:4599–4606.
 35. **Teglund, S., C. McKay, E. Schuetz, J. M. van Deursen, D. Stravopodis, D. Wang, M. Brown, S. Bodner, G. Grosfeld, and J. N. Ihle.** 1998. Stat5a and Stat5b proteins have essential and nonessential, or redundant, roles in cytokine responses. *Cell* **93**:841–850.
 36. **Tollet-Egnell, P., A. Flores-Morales, N. Stahlberg, R. L. Malek, N. Lee, and G. Norstedt.** 2001. Gene expression profile of the aging process in rat liver: normalizing effects of growth hormone replacement. *Mol. Endocrinol.* **15**:308–318.
 37. **Udy, G. B., R. P. Towers, R. G. Snell, R. J. Wilkins, S. H. Park, P. A. Ram, D. J. Waxman, and H. W. Davey.** 1997. Requirement of STAT5b for sexual dimorphism of body growth rates and liver gene expression. *Proc. Natl. Acad. Sci. USA* **94**:7239–7244.
 38. **VanderKuur, J. A., X. Wang, L. Zhang, G. S. Campbell, G. Allevalo, N. Billestrup, G. Norstedt, and C. Carter-Su.** 1994. Domains of the growth hormone receptor required for association and activation of JAK2 tyrosine kinase. *J. Biol. Chem.* **269**:21709–21717.
 39. **Wang, Y. D., K. Wong, and W. I. Wood.** 1995. Intracellular tyrosine residues of the human growth hormone receptor are not required for the signaling of proliferation or Jak-STAT activation. *J. Biol. Chem.* **270**:7021–7024.
 40. **Waters, M. J., and H. G. Friesen.** 1979. Purification and partial characterization of a nonprimate growth hormone receptor. *J. Biol. Chem.* **254**:6815–6825.
 41. **Woelfle, J., D. J. Chia, and P. Rotwein.** 2003. Mechanisms of growth hormone (GH) action. Identification of conserved Stat5 binding sites that mediate GH-induced insulin-like growth factor-I gene activation. *J. Biol. Chem.* **278**:51261–51266.
 42. **Wu, H., X. Liu, and R. Jaenisch.** 1994. Double replacement: strategy for efficient introduction of subtle mutations into the murine Col1a-1 gene by homologous recombination in embryonic stem cells. *Proc. Natl. Acad. Sci. USA* **91**:2819–2823.
 43. **Yuferov, V., T. Krosiak, K. S. Laforge, Y. Zhou, A. Ho, and M. J. Kreek.** 2003. Differential gene expression in the rat caudate putamen after “binge” cocaine administration: advantage of triplicate microarray analysis. *Synapse* **48**:157–169.
 44. **Zang, H., K. Sato, H. Nakajima, C. McKay, P. A. Ney, and J. N. Ihle.** 2001. The distal region and receptor tyrosines of the Epo receptor are nonessential for in vivo erythropoiesis. *EMBO J.* **20**:3156–3166.
 45. **Zhou, Y., B. C. Xu, H. G. Maheshwari, L. He, M. Reed, M. Lozykowski, S. Okada, L. Cataldo, K. Coschigano, T. E. Wagner, G. Baumann, and J. J. Kopchick.** 1997. A mammalian model for Laron syndrome produced by targeted disruption of the mouse growth hormone receptor/binding protein gene (the Laron mouse). *Proc. Natl. Acad. Sci. USA* **94**:13215–13220.

ERRATUM

In Vivo Analysis of Growth Hormone Receptor Signaling Domains and Their Associated Transcripts

Jennifer E. Rowland, Agnieszka M. Lichanska, Linda M. Kerr, Mary White,
Elisabetta M. d'Aniello, Sheryl L. Maher, Richard Brown, Rohan D. Teasdale,
Peter G. Noakes, and Michael J. Waters

Institute for Molecular Bioscience and School of Biomedical Sciences, University of Queensland, St. Lucia, Queensland, Australia

Volume 25, no. 1, p. 66–77, 2005. Page 67, Fig. 1D: The middle and right lanes of the top panel should be labeled “569–/+” and “569,” respectively, and the middle lane of the bottom panel should be labeled “391–/+.”